Decentralized Optimal Dispatch of Reactive Power Sources in Power Systems Based on Augmented Lagrangian Method

Hoa M. Nguyen*, Tien N. Nguyen**, and Hoan V. Pham*‡

*Department of Electrical Engineering, Tra Vinh University, Vietnam

(hoatvu@tvu.edu.vn, pham.v.hoan@tvu.edu.vn)

**Department of Electrical Engineering, Can Tho University, Vietnam

(nntien@ctu.edu.vn)

‡ Corresponding Author: Hoan V. Pham, Department of Electrical Engineering, Tra Vinh University, Vietnam, Tel: +84 294 3855246,

Fax: +84 294 3855217, pham.v.hoan@tvu.edu.vn

Received: 20.03.2022 Accepted: 26.04.2022

Abstract- This paper proposes a sensitivity matrix-based formulation methodology for decentralized optimal reactive power dispatch problems on multi-region interconnected power systems. A large power system is divided into multi-region, with region operators agreeing on the progression of variables and determining optimal local control variables using the local system model and a communication network with its adjacent control regions. The constrained objective function is substituted with a sequence of unconstrained sub-problems using the augmented Lagrangian approach to achieve global optimization. To specify control variables, such as reactive power injections, and transformer tap positions, a linearized objective function with a set of local constraints must be addressed in each region. A nonlinear optimization algorithm using function *fmincon* in Matlab is utilized to solve the mathematical model effectively and is applied to the modified IEEE 30-bus system to demonstrate the validity and effectiveness of the proposed method.

Keywords - Decentralized optimization; multi-region interconnected power system; network partitioning; reactive power dispatch; voltage control.

1. Introduction

As a sub-problem of optimal power flow (OPF), the optimal reactive power dispatch (ORPD) problem significantly improves the system security, voltage profile, power transfer capability, and overall network efficiency. The ORPD's goal is to fine-tune the control variables to achieve permissible voltage profiles and minimal power losses while lowering operational costs **Hata! Başvuru kaynağı bulunamadı.**. By minimizing the real power loss, the ORPD helps to reduce the system congestion. And adjusting transformer tap settings, generator voltages, and reactive power sources like flexible alternating current transmission systems (FACTS) are all part of this strategy. The power system operators are in charge of operating and maintaining the system voltage profile, hence requiring a sufficient amount of reactive power to manage voltage violations in the transmission grid **Hata! Başvuru kaynağı bulunamadı.**,[3]. In typical circumstances, both the voltage profile and the active power losses are determined by the system's reactive power. Active power losses minimization must be considered a substantial goal when operating a power system efficiently **Hata! Başvuru kaynağı bulunamadı.**–**Hata! Başvuru kaynağı bulunamadı.**. As a result, regional operators must coordinate control operations while remaining local information relevant to system infrastructure undisclosed [12]. The objective function (OF) in this paper is the minimization of the transmission power losses while ensuring that the voltage remains within permissible limits.

Various studies have been made to address the ORPD by using centralized approaches, namely the centralized optimal reactive power dispatch (C-ORPD). These approaches have a significantly increased requirement of computation, storage resources, and communication bandwidth along with the size of power systems. Furthermore, the system data are gathered and processed by the operation center; therefore, the data of all regions must be exposed. As a result, the traditional centralized optimization is inapplicable to the multi-region interconnected power systems. The distributed optimization method known as fast calculation speed, high robustness, and the decomposition capability is a suitable solution to the multi-region optimization problem. This paper presents a distributed optimization scheme using the Lagrangian decomposition algorithm and augments the OF by including global optimization of linearized multi-area power systems **Hata! Başvuru kaynağı bulunamadı.**–**Hata! Başvuru kaynağı bulunamadı.**. The goal is to keep centralized coordination among regions, considering loss reduction as investigated distributed optimization while safeguarding each region's important data. Each region's OF efficiency is due to the application of sensitivity of active power loss to the system's control variables. In the initial stages, sensitivities of the loss to the control variables are employed, which are generated using the linearized system model **Hata! Başvuru kaynağı bulunamadı.**, [17]. Finally, this paper addresses a centralized optimization problem using the decomposition approach.

The classical technique for tackling constrained optimization problems is lagrangian decomposition. The augmented Lagrangian approach simulates a Lagrange multiplier by adding the term to the unconstrained objective [18]. This method has been widely utilized to solve various engineering problems, particularly in the field of power systems **Hata! Başvuru kaynağı bulunamadı.**–**Hata! Başvuru kaynağı bulunamadı.**. The benefit of this method is that local grid data remains confidential. However, because it takes iterating several times to reach the optimization, it degrades computational efficiency.

Strategies using nonlinear power flow (PF) equations in solving the ORPD are frequently used; however, they usually suffer from a significant computation burden due to repetition of the PF calculation, making them unsuitable for real-time applications [13]. To overcome this shortcoming, the ORPD problem is formulated by using sensitivity analysis in this paper.

In this paper, the augmented Lagrangian technique was developed and studied using loss minimization as the OF. An unique formulation employing sensitivity analysis to characterize the decentralized optimal reactive power dispatch (D-ORPD) is presented. Not only can our method handle decentralized problems of optimal reactive power dispatch, but it can also tackle decentralized real-time computing difficulties in the multi-region interconnected power systems. Furthermore, the D-ORPD employing the proposed formulation is applied on a modified IEEE 30-bus system, and the control scheme's performance has been investigated for numerous scenarios, followed by a conclusion.

2. The RPD Problem's Formulation

2.1. Objective Function

A formulation of the D-ORPD problem is proposed in this study to deal with the inequality constraints and reduce active power losses across the power grid. The objective function J is loss minimization, and the voltage profile is allowed from 0.9 to 1.1 p.u. Sensitivities achieved by linearizing the PF equations are used to introduce the OFs in (2) in a linearized form. Changes in the control variables $\Delta \boldsymbol{w}_i(k)$ are obtained by minimizing the OFs (2).

$$\min \mathrm{J} = \sum_{i=1}^{N^a} \mathrm{J}_i \tag{1}$$

$$\mathrm{J}_i = \left(\left(\frac{\partial P_i^{loss}}{\partial \boldsymbol{w}_i} \right) \Delta \boldsymbol{w}_i(k) \right) \tag{2}$$

$$\boldsymbol{w}_i = \left[\left[\boldsymbol{u}_i \right]^T, \left[\boldsymbol{v}_{ij}^{'} \right]^T \right]^T \tag{3}$$

where N^a is the number of control regions in the interconnected power system, $\partial P_i^{loss} / \partial \boldsymbol{w}_i$ and $\partial v_i / \partial \boldsymbol{w}_i$ are sensitivities of the loss and the voltage to control variables of the region *i*, respectively, and $v_{ij}^{'}$ is voltage magnitude at boundary nodes, linked to the region *i*, of adjacent regions *j* which is desired by the region *i*. $\boldsymbol{u}_i$ represent control variables of the region *i*.

The sensitivities in the D-ORPD can be calculated in two layers, as shown in (4).

$$\frac{\partial P_i^{loss}}{\partial \boldsymbol{w}_i} = \frac{\partial P_i^{loss}}{\partial \boldsymbol{v}_i} \frac{\partial \boldsymbol{v}_i}{\partial \boldsymbol{w}_i} \tag{4}$$

According to the number of branches N_{br} of the region *i*, the active power loss P_i^{loss} of region *i* is presented by

$$P_i^{loss} = \sum_{k=1}^{\mathrm{N_{br}}} \mathrm{G}_k [v_a^2 + v_b^2 - 2 v_a v_b \cos(\delta_a - \delta_b)] \tag{5}$$

where G_k is the branch *k*'s conductance which links buses *a* to *b*.

The equation (4) is then used to calculate the partial derivatives of P_i^{loss} to the voltages at nodes *a* and *b* as follows:

$$\frac{\partial P^{loss}}{\partial v_a} = \mathrm{G}_k [2 v_a - 2 v_b \cos(\delta_a - \delta_b)] \tag{6}$$

$$\frac{\partial P^{loss}}{\partial v_b} = \mathrm{G}_k[2v_b - 2v_a\cos(\delta_a - \delta_b)] \tag{7}$$

The sensitivities of the loss to all node voltages in the system are formed by adding partial derivatives for each bus.

The control variables' vector $\boldsymbol{w}_i$ is the result of combining the inter-region variables $\boldsymbol{v}_{ij}^{'}$, generator reactive power injection $\boldsymbol{q}_{g,i}$, and tap ratio $\boldsymbol{\alpha}_{tap,i}$. As a result, the second layer was defined by calculating 03 sensitivities: $\partial\boldsymbol{v}_i / \partial\boldsymbol{v}_{ij}^{'}$, $\partial\boldsymbol{v}_i / \partial\boldsymbol{q}_{g,i}$, and $\partial\boldsymbol{v}_i / \partial\boldsymbol{\alpha}_{tap,i}$.

It is obvious that $\partial\boldsymbol{v}_i / \partial\boldsymbol{v}_{ij}^{'}$ is a unity vector and $\partial\boldsymbol{v}_i / \partial\boldsymbol{q}_{g,i}$ is the Jacobian matrix inversion calculated below:

Injection of reactive power into bus k

$$q_k = v_k \sum_{m=1}^{\mathrm{N_{bus}}} (\mathrm{G}_{km} v_m \sin\theta_{km} - \mathrm{B}_{km} v_m \cos\theta_{km}) \tag{8}$$

Then the Jacobian matrix is structured in the following way:

$$J_{km} = \frac{\partial q_k}{\partial v_m} = v_k(\mathrm{G}_{km}\sin\theta_{km} - \mathrm{B}_{km}\cos\theta_{km}) \tag{9}$$

$$\begin{aligned} J_{kk} = \frac{\partial q_k}{\partial v_k} &= 2v_k(\mathrm{G}_{kk}\sin\theta_{kk} - \mathrm{B}_{kk}\cos\theta_{kk}) \\ &+ \sum_{m=1, m\neq k}^{\mathrm{N_{bus}}} v_m(\mathrm{G}_{km}\sin\theta_{km} - \mathrm{B}_{km}\cos\theta_{km}) \end{aligned} \tag{10}$$

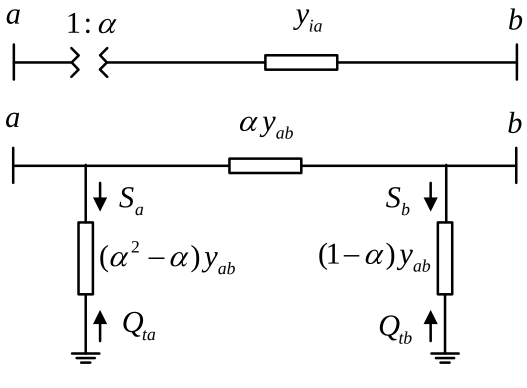

Fig. 1. Equivalent π circuit for the tap changing transformer

Changing the transformer's tap ratio is equal to injecting two reactive power sources into the transformer terminals in this paper. As a result, the sensitivities $\partial\boldsymbol{v}_i / \partial\boldsymbol{\alpha}_{tap,i}$ are comparable to the following two levels of sensitivities:

$$\frac{\partial\boldsymbol{v}_i}{\partial\boldsymbol{\alpha}_{tap,i}} = \frac{\partial\boldsymbol{v}_i}{\partial\boldsymbol{q}_{tap,i}} \frac{\partial\boldsymbol{q}_{tap,i}}{\partial\boldsymbol{\alpha}_{tap,i}} \tag{11}$$

The sensitivities $\partial\boldsymbol{v}_i / \partial\boldsymbol{q}_{tap,i}$ are a sub-matrix of the $\partial\boldsymbol{v}_i / \partial\boldsymbol{q}_{g,i}$. While $\partial\boldsymbol{v}_i / \partial\boldsymbol{\alpha}_{tap,i}$ is calculated as follows:

Due to the direct involvement of two nodes in the tap changing process, transformer tap change is more challenging to simulate. Consider the transformer in Figure 1 that connects nodes a and b with a tap α. An equivalent π circuit can be used to represent this branch.

The branch admittance is:

$$y_{ab} = g_{ab} + jb_{ab} \tag{12}$$

From **Hata! Başvuru kaynağı bulunamadı.**1, the injection of complex power to node a is

$$s_a = p_a + jq_a = v_a i_a^* = v_a\left[v_a(\alpha^2 - \alpha)y_{ab}\right]^* \tag{13}$$

where * shows the complex conjugate. Hence,

$$s_a = v_a^2(\alpha^2 - \alpha)g_{ab} - jv_a^2(\alpha^2 - \alpha)b_{ab} \tag{14}$$

Similarly, node b is shown as

$$s_l = v_l^2(1-\alpha)g_{ab} - jv_b^2(1-\alpha)b_{ab} \tag{15}$$

From equations (14) and (15), we have

$$q_a = -v_a^2(\alpha^2 - \alpha)b_{ab} \tag{16}$$

$$q_b = -v_b^2(1-\alpha)b_{ab} \tag{17}$$

If Δq_a is the change of q_a in regards to tap position and voltage changes, then

$$\Delta q_a = \frac{\partial q_a}{\partial v_a}\Delta v_a + \frac{\partial q_a}{\partial \alpha}\Delta\alpha \tag{18}$$

However, for the PF in **Hata! Başvuru kaynağı bulunamadı.**, we have

$$\Delta q_{ta} = -\Delta q_a \tag{19}$$

So, differentiating (16) with respect to v_a and α,

$$\Delta q_{ta} = 2b_{ab}v_a(\alpha^2 - \alpha)\Delta v_a + b_{ab}v_a^2(2\alpha - 1)\Delta\alpha \tag{20}$$

Similarly, differentiating (17) with respect to v_b and α

$$\Delta q_{tb} = 2b_{ab}v_b(1-\alpha)\Delta v_b - b_{ab}v_b^2\Delta\alpha \tag{21}$$

Equation (20) can also be rewritten:

$$\begin{aligned} \Delta q_{ta} &= 2b_{ab}v_a\alpha(\alpha - 1)\Delta v_a \\ &+ b_{ab}v_a^2(\alpha - 1)\Delta\alpha + b_{ab}v_a^2\alpha\Delta\alpha \end{aligned} \tag{22}$$

Since α is close to unity, Δv_a and $\Delta\alpha$ are small, therefore

$$\frac{\Delta q_{ta}}{\Delta\alpha} = b_{ab} v_a^2 \alpha \tag{23}$$

In the same way, from equation (21),

$$\frac{\Delta q_{tb}}{\Delta\alpha} = -b_{ab} v_b^2 \tag{24}$$

2.2. Constraints

$$\boldsymbol{v}_{ij}^{'} = \boldsymbol{v}_{ji} \tag{25}$$

$$\Delta\boldsymbol{w}_i^{\min} \le \Delta\boldsymbol{w}_i(k) \le \Delta\boldsymbol{w}_i^{\max} \tag{26}$$

$$\Delta\mathbf{v}_i^{\min} \le \Delta\boldsymbol{v}_i(k+1) \le \Delta\mathbf{v}_i^{\max} \tag{27}$$

$$\mathbf{v}_i^{\min} \le \boldsymbol{v}_i(k+1) \le \mathbf{v}_i^{\max} \tag{28}$$

$$\boldsymbol{v}_i(k+1) = \boldsymbol{v}_i(k) + \left(\frac{\partial\boldsymbol{v}_i}{\partial\boldsymbol{w}_i}\right)_D \Delta\boldsymbol{w}_i(k) \tag{29}$$

where $\mathbf{v}_i^{max}$ and $\mathbf{v}_i^{min}$ are the maximum and minimum of voltages that are permitted in region *i* respectively. The aforementioned equations' constraints are the result of linearizing the PF equations. They depict voltage limitations, reactive power injections through devices, and transformer tap-positions. The regional operators would analyze and re-calibrate these parameters after each local optimization.

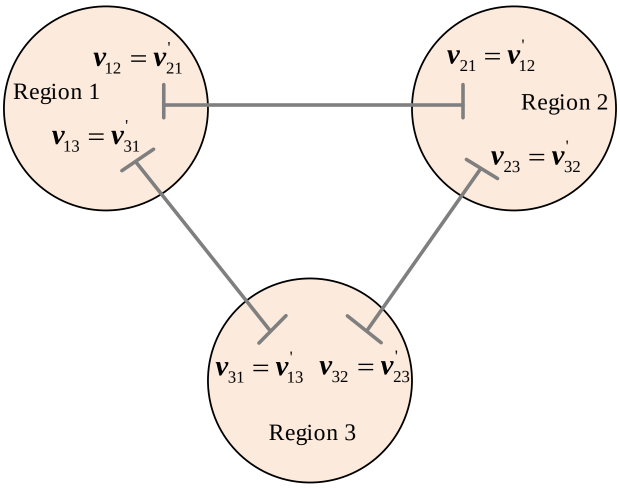

Fig. 2. Multi-regions interconnected power system managed by decentralized algorithm based system

In real-world circumstances, power systems cover thousands of kilometers, sometimes even countries and continents, mostly for the sake of improved use, efficiency, and management. When these regions are divided into several regions, each operated by a local operator, a network of numerous operators with local control emerges. For a system to be efficient and reliable, these operators must communicate with one another. Nonetheless, regional data such as reactive power reserves, power generation capacity, and infrastructural details, among other things, must be safeguarded against one another. Assume $\boldsymbol{v}_{ji}$ is the magnitude of the voltage at these buses, but is expected by its region *j*. Achieving consensus in these locations entails negotiating the voltage profile at the tie-lines, as shown in equation (25). The regions are connected via tie-lines or linking buses, as shown in Figure 2, and the voltages $\boldsymbol{v}_{ij}$ solution to the previous equations for N^a regions regulate the entire system.

3. Augmented Lagrange Method

The augmented Lagrangian methods have obtained large attention in the recent past for solving constrained global optimization problems. In the same way that penalty methods replace a constrained optimization problem with a set of unconstrained problems and add a penalty term to the OF, the augmented Lagrangian techniques add yet another term, aiming to simulate a Lagrange multiplier. The augmented Lagrangian is similar to, but not identical to, the Lagrangian multiplier approach.

Due to the boundary constraints, the overall control problems (1)–(3) and (25)–(29) cannot be divided into sub-problems utilizing the variables of the region *i* only. As a result, in this section, a distributed algorithm based on the augmented Lagrangian method is developed and presented to deal with the global OF of the entire system by addressing local problems independently.

To integrate the boundary constraints of equation (25) into the global goal function (1), the augmented Lagrangian technique is employed. The global goal, as well as the losses and inter-region constraints, can now be displayed in (30).

$$L(\boldsymbol{\Lambda}) = \sum_{i=1}^{N^a} \begin{pmatrix} J_i + \sum_{j\in N_i} (\boldsymbol{\lambda}_{ij})^T (\boldsymbol{v}_{ij}^{'} - \boldsymbol{v}_{ij}) \\ + \frac{\rho}{2} \left\| \boldsymbol{v}_{ij}^{'} - \boldsymbol{v}_{ij} \right\|_2^2 \end{pmatrix} \tag{30}$$

with constraints ranging from (26) to (29) and a penalty parameter ρ penalizing interconnecting constraint breaches.

Then the equation (30) is rewritten in the form of individual sub-problems

$$\min_{\boldsymbol{w}_i, \boldsymbol{v}_{ij}^{'}} \begin{pmatrix} \mathrm{J}_i + \sum_{j\in \mathrm{N}_i} \left(\left[(\boldsymbol{\lambda}_{ij})^{\mathrm{T}} \;\; (-\boldsymbol{\lambda}_{ji})^{\mathrm{T}} \right] \begin{bmatrix} \boldsymbol{v}_{ij}^{'} \\ \boldsymbol{v}_{ij} \end{bmatrix} \right. \\ \left. + \frac{\rho}{2} \left\| \begin{bmatrix} \mathrm{I} & 0 \\ 0 & \mathrm{I} \end{bmatrix} \begin{bmatrix} \boldsymbol{v}_{ji,prev}^{'} \\ \boldsymbol{v}_{ji,prev} \end{bmatrix} - \begin{bmatrix} 0 & \mathrm{I} \\ \mathrm{I} & 0 \end{bmatrix} \begin{bmatrix} \boldsymbol{v}_{ij}^{'} \\ \boldsymbol{v}_{ij} \end{bmatrix} \right\|_2^2 \right) \end{pmatrix} \tag{31}$$

where the subscript *prev* denotes the value of the variables at the previous iteration step.

Figure 3 depicts the algorithm for implementing the augmented Lagrangian method. To identify the optimal local and boundary variables, each region first updates its sensitivity and then minimizes its issue (31) while unchanging the variables of the other regions. After the last region finishes solving its sub-problem, termination requirements such as the condition on the maximum permissible number of iterations in (34) or the boundary variables in (35) are checked. The selected actions are carried out if the requirements are met. In the case of the requirements unfulfilled, the equations (32) and (33) are used to update the Lagrangian multipliers, and the procedure is repeated.

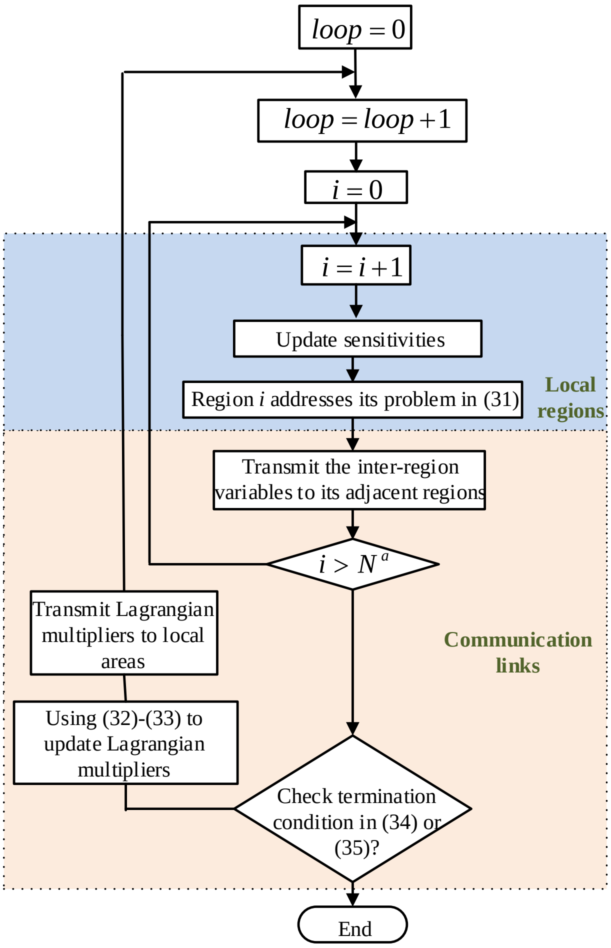

Fig. 3. Flow chart of implementation algorithm

$$\lambda_{ij} = \lambda_{ij} + \rho\left(v'_{ij} - v_{ji}\right) \tag{32}$$

$$\lambda_{ji} = \lambda_{ji} + \rho\left(v'_{ji} - v_{ij}\right) \tag{33}$$

$$loop \le loop^{\max} \tag{34}$$

$$v'_{ij} - v_{ji} < \varepsilon^{v} \tag{35}$$

with $\forall i, j \in N^a$

4. Simulation Results

4.1. Test System

The proposed method was tested using a modified IEEE 30-bus system from [22]. As illustrated in Figure 4, the test system is divided into three sections, totaling 10 tap-changer equipped transformers, each with 02 generators and multiple loads. There are seven tie-lines, which correlate to fourteen boundary variables. Table 1 gives the details of the partitioning of the IEEE 30-bus system. It also gives details on the number of boundary buses and tie lines present in each system.

Table 1. Details of the IEEE 30-bus system and its partitioning

No. of nodes	30
No. of regions	3
No. of transformers	10
Nodes in each region	11, 10, 9
No. of tie-lines	7
Boundary nodes in each region	3, 4, 3

4.2. Simulation Process

The simulation results displayed below are based on Table 2's control parameters. They are divided into global parameters that apply to the global optimization and augmented Lagrangian parameters that apply to the augmented Lagrangian approach.

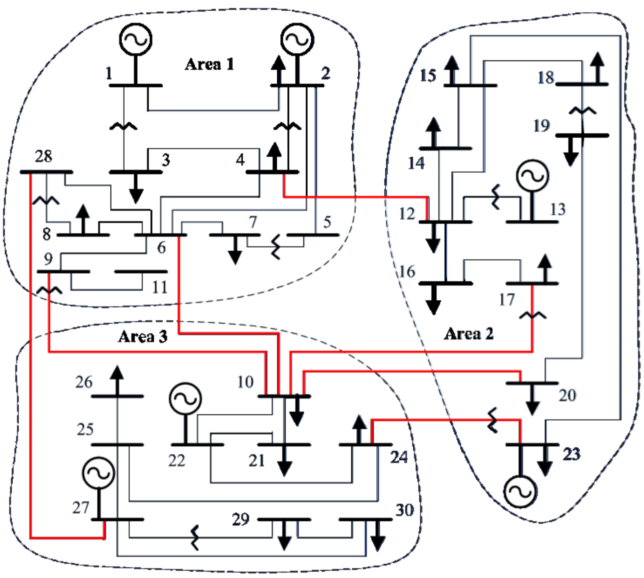

Fig. 4. Modified IEEE 30-bus test system.

A larger N_{step} may imply stronger performance but also a greater computational load. In this case, $N_{step} = 4$ is chosen intuitively. Furthermore, it is expected that the controller's calculating time to provide values of the control variables is within 2 seconds.

4.2.1. Performance comparison between decentralized method and centralized method

Figure 5 shows that the centralized method delivers a greater convergence value of the losses compared to the decentralized method. This is most likely since the greater the ε^{v} value of the consensus on boundary variables in (34) is, the poorer the performance of reducing losses. Moreover, the convergence speed of the centralized method is quicker.

Furthermore, the simulation results demonstrate the potential of the proposed control algorithm in promoting regional collaboration to attain the global goal. Figure 5 shows that the loss in region 3 (D-Region 3) shows a trend toward a rise from the control circle 12, whereas the losses in other regions fall and the entire system reduces in response.

Table 2. Setup parameters

Global parameters	ε_i^{loss} (MW)	0.01
	$\lvert\Delta \boldsymbol{v}_i^{\max}\rvert$ & $\lvert\Delta \boldsymbol{v}_i^{\min}\rvert$ (p.u.)	0.03
	$\lvert\Delta \boldsymbol{q}_i^{\max}\rvert$ & $\lvert\Delta \boldsymbol{q}_i^{\min}\rvert$ (p.u.)	0.02
	$\lvert\Delta \boldsymbol{\alpha}_i^{\max}\rvert$ & $\lvert\Delta \boldsymbol{\alpha}_i^{\min}\rvert$ (p.u.)	0.002
Parameters of multi-regions system	ε^{v} (p.u.)	0.0005
	ρ	9.5
	$loop^{\max}$	300

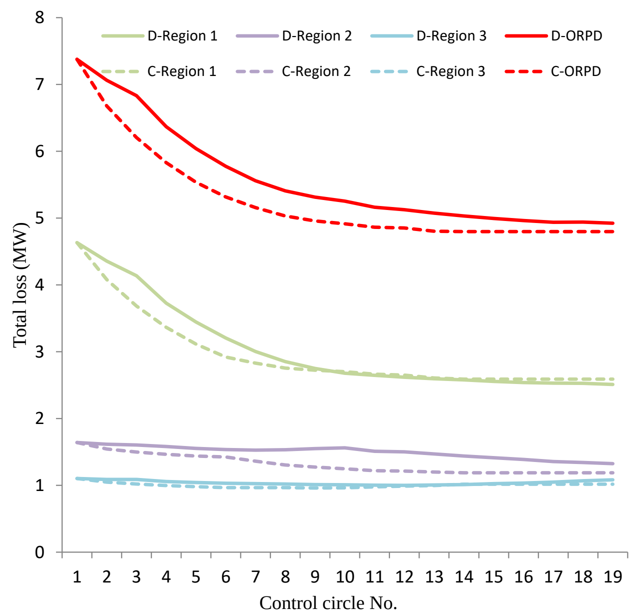

Fig. 5. Comparative convergence profiles of power loss between centralized and decentralized methods

4.2.2. Effects of global parameters on the control performance

To investigate the effects of control settings on performance, we simulate each scenario below with only one of the parameters altered while keeping the other parameters fixed. The settings are presented in Table 2.

Figure 6 shows loss convergence for various voltages with varied change limits. The narrower constraints, as illustrated below, result in a slower convergence speed but a higher convergence value within the first control circles, which is far from optimal. Because the algorithm performance is inversely proportional to the limitations, significant limits frequently cause the convergence value to fluctuate, increasing the probability of triggering the termination condition (34).

As shown in Figures 7 and 8, the greater change in magnitudes of control variables may harm the algorithm's performance. It is obvious since calculated sensitivities are utilized for modest changes in control variables.

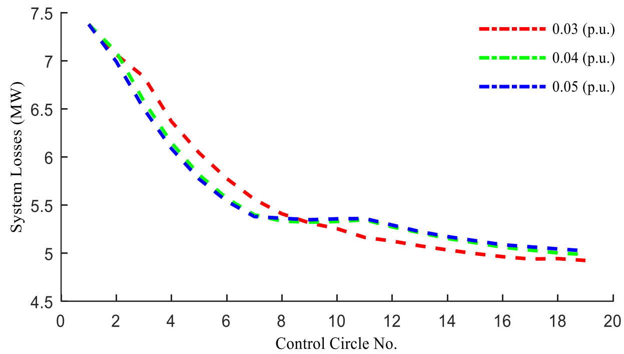

Fig. 6. Convergence of losses with varied voltage limits $\lvert\Delta \mathbf{v}_i^{max}\rvert = \lvert\Delta \mathbf{v}_i^{min}\rvert$

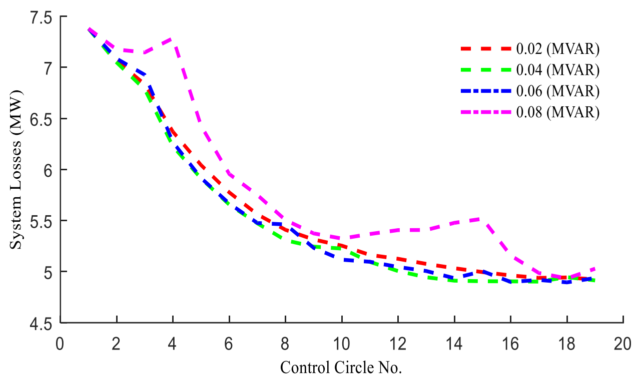

Fig 7. Convergence of losses with varying reactive power injection limits from generators

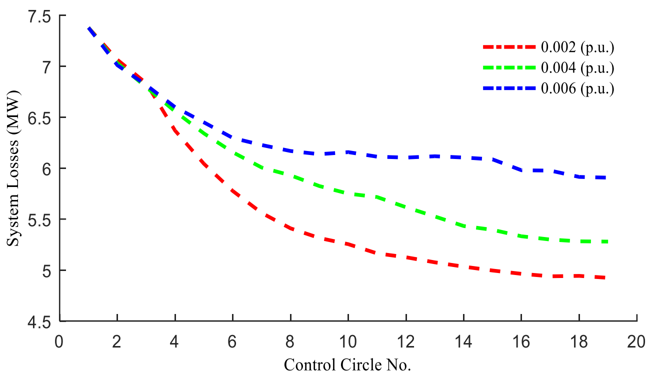

Fig. 8. Loss convergence with varied tap movement limits

4.2.3. Effects of multi-region parameters on the performance

It appears that selecting the suitable value of the penalty parameter ρ to get the best performance is very challenging, as shown in Figure 9. Furthermore, it should be noted that the penalty parameter ρ is strongly related to the performance of the control scheme.

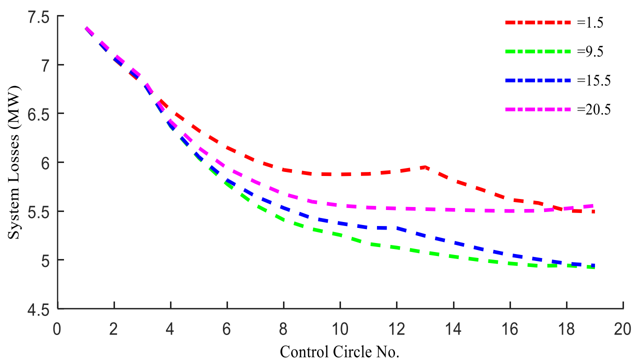

Fig. 9. Loss convergence with different penalty parameter ρ

5. Conclusions

In this paper, a novel formulation of the D-ORDP based sensitivity analysis is presented to enable the decentralized optimization method. The idea for a decentralized method-based system came from the necessity for protection and coordination of sensitive data in vast interconnected power systems for reliable power system operation. Loss minimization was used as the OF to build and analyze an effective augmented Lagrange decomposition technique. As shown in the simulation results, the proposed strategy not only safeguards local data but also can be comparable to the traditional centralized method. While the centralized method achieves a better loss convergence value, the proposed control algorithm is shown to promote regional collaboration in order to achieve the global goal.

Improper control setting selection, on the other hand, decreases performance. In this paper, these parameters were chosen by trial and error, however precise estimation of these parameters will help to reduce computation time and improve the algorithm's performance. Furthermore, due to its reliance on the updating of the Lagrangian multipliers, the augmented Lagrange decomposition approach has the drawback of no longer being separable across subsystems. We can instead employ the alternating direction method of multipliers, which has been widely adopted in numerous industries due to its ease of decomposition and convergence guarantees on a wide variety of problems, to accomplish both separability and robustness for distributed optimization.

Acknowledgements

This study was fully funded by Tra Vinh University under the project contract No. 212/HĐ.HĐKH- ĐHTV dated on September 16, 2019.

References

[1] M. Ebeed, A. Alhejji, S. Kamel and F. Jurado, “Solving the optimal reactive power dispatch using marine predators algorithm considering the uncertainties in load and wind-solar generation systems,” *Energies*, vol. *13*, no. 17, Aug. 2020.

[2] V.H. Pham, J.L. Rueda, and I. Erlich, “Online optimal control of reactive sources in wind power plants”, *IEEE Transactions on Sustainable Energy*, vol. 5, no. 2, pp. 608–616, Aug. 2013.

[3] K. Li, X. Han, W. Li and R. Ahmed, "Unified power flow algorithm of transmission and distribution network," *2017 IEEE 6th International Conference on Renewable Energy Research and Applications (ICRERA)*, pp. 257-261, 2017.

[4] T.M. Beza, Y-C Huang, and C-C Kuo, “A hybrid optimization approach for power loss reduction and DG penetration level increment in electrical distribution network”, *Energies*, vol. 13, no. 6008, Nov. 2020.

[5] Hoa M. Nguyen, J.L. Rueda Torres, A. Lekíc, and Hoan V. Pham, “MPC based centralized voltage and reactive power control for active distribution networks*”, IEEE Trans. Energy Conversion*, vol. 36, no. 2, pp. 1537-1547, June 2021.

[6] Y. Ai, M. Du, Z. Pan and G. Li, "The optimization of reactive power for distribution network with PV generation based on NSGA-III," *CPSS Transactions on Power Electronics and Applications*, vol. 6, no. 3, pp. 193-200, Sept. 2021.

[7] N. H. Khan, Y. Wang, D. Tian, M. A. Z. Raja, R. Jamal and Y. Muhammad, "Design of Fractional Particle Swarm Optimization Gravitational Search Algorithm for Optimal Reactive Power Dispatch Problems," *IEEE Access*, vol. 8, pp. 146785-146806, 2020.

[8] Y. Chai, L. Guo, C. Wang, Y. Liu and Z. Zhao, "Hierarchical Distributed Voltage Optimization Method for HV and MV Distribution Networks," *IEEE Transactions on Smart Grid*, vol. 11, no. 2, pp. 968-980, March 2020.

[9] G.A. Ajenikoko, A.W. Eboda, and T.S. Adeyemi, “A genetic algorithm approach for optimal distribution system network reconfiguration”, *International Journal*

of Smart Grid (ijSmartGrid), vol. 1, no. 1, September 2017.

[10] S. Ermis, M. Yesilbudak and R. Bayindir, "Optimal power flow using artificial bee colony, wind driven optimization and gravitational search algorithms," *2019 8th International Conference on Renewable Energy Research and Applications (ICRERA)*, pp. 963-967, 2019.

[11] S. Alshahrani, M. Al-Muhaini and M. Khalid, "Minimizing active/reactive power losses in electricity networks based on optimal location of battery energy storage system," *2019 8th International Conference on Renewable Energy Research and Applications (ICRERA)*, pp. 287-294, 2019.

[12] W. Lu, M. Liu, S. Lin, and L. Li, "Fully decentralized optimal power flow of multi-region interconnected power systems based on distributed interior point method", *IEEE Trans. Power Syst.*,, vol. 33, no. 1, pp. 901-910, Jan. 2018.

[13] S. Boyd and L. Vandenberghe, Convex Optimization, Cambridge University Press, Cambridge, United Kingdom, 2004.

[14] D. P. Bertsekas, Constrained Optimization and Lagrange Multiplier Methods, Academic Press, London, UK, 1982.

[15] G. Fusco, M. Russo, and M. De Santis, "Decentralized voltage control in active distribution systems: Features and open issues," *Energies*, vol. *14*, no. 2563, April 2021.

[16] P. C. Maduforo, J.N. Emechebe, E.M. Eronu, and S.A. Benson, "Sensitivity base approach for the optimal sizing and allocation of distributed generation in a radial network," *European Journal of Engineering and Science*, vol. *5*, no. 6, June 2020.

[17] M. Khayamy, A. Nasiri, and F. Balali, "Analytical study based optimal placement of energy storage devices in power systems to support voltage and angle stability," *International Journal of Smart Grid*, vol. *3*, no. 4, Dec. 2019.

[18] W. Ananduta, C. Ocampo-Martinez, and A. Nedíc, "A distributed augmented Lagrangian method over stochastic networks for economic dispatch of large-scale energy systems", *IEEE Trans. Sustainable Energy*, vol. 12, no. 4, pp. 1927-1934, Oct. 2021.

[19] Y. Zhang, and M. Zavlanos, "A consensus-based distributed augmented Lagrangian method," in Proc. of IEEE Conference on Decision and Control, Miami Beach, USA, 2018.

[20] T. Muhlpfordt, X. Dai, A. Engelmann, and V. Hagenmeyer, "Distributed power flow and distributed optimization – Formulation, solution, and open-source implementation," *Elsevier*, vol. 26, June 2021.

[21] Z. Hou, H.C. Wu, and S.C. Chan, "Distributed optimal power flow: An augmented Lagrangian-sequential quadratic programming approach," in Proc. of IEEE International Symposium on Circuits and Systems, Baltimore, MD, USA, 2017.

[22] N. I. Deeb and S. M. Shahidehpour, "An efficient technique for reactive power dispatch using a revised linear programming approach," *Electr. Power Syst. Res.*, vol. 15, no. 2, pp. 121–134, 1988.